Chinese Herbal Medicines 17 (2025) 178–188

Contents lists available at ScienceDirect

Chinese Herbal Medicines

journal homepage: www.elsevier.com/locate/chmed

Original Article

Metabolome and transcriptome association study reveals biosynthesis of specialized benzylisoquinoline alkaloids in *Phellodendron amurense*

Tingxia Liu [a,b,1], Wanran Zhang [c,1], Sijia Wang [a,b], Ya Tian [c], Yifan Wang [c], Ranran Gao [b], Shilin Chen [b], Wei Sun [b], Wei Ma [a,*], Zhichao Xu [c,*]

[a] College of Pharmaceutical Sciences, Heilongjiang University of Chinese Medicine, Harbin 150040, China
[b] Key Laboratory of Beijing for Identification and Safety Evaluation of Chinese Medicine, Institute of Chinese Materia Medica, China Academy of Chinese Medical Sciences, Beijing 100700, China
[c] College of Life Sciences, Northeast Forestry University, Harbin 150040, China

ARTICLE INFO

Article history:
Received 16 April 2024
Revised 24 September 2024
Accepted 7 November 2024
Available online 9 November 2024

Keywords:
benzylisoquinoline alkaloids
biosynthesis
evolution
norcoclaurine synthase
Phellodendron amurense Rupr

ABSTRACT

Objective: Benzylisoquinoline alkaloids (BIAs) have pharmacological functions and clinical use. BIAs are mainly distributed in plant species across the order Ranunculales and the genus *Phellodendron* from Sapindales. The BIA biosynthesis has been intensively investigated in Ranunculales species. However, the accumulation mechanism of BIAs in *Phellodendron* is largely unknown. The aim of this study is to unravel the biosynthetic pathways of BIAs in *Phellodendron amurens*.

Methods: The transcriptome and metabolome data from 18 different tissues of *P. amurense* were meticulously sequenced and subsequently subjected to a thorough analysis. Weighted gene co-expression network analysis (WGCNA), a powerful systems biology approach that facilitates the construction and subsequent analysis of co-expression networks, was utilized to identify candidate genes involved in BIAs biosynthesis. Following this, recombinant plasmids containing candidate genes were expressed in *Escherichia coli*, a widely used prokaryotic expression system. The purpose of this genetic engineering endeavor was to express the candidate genes within the bacteria, thereby enabling the assessment of the resultant enzyme activity.

Results: The synonymous substitutions per synonymous site for paralogs indicated that at least one whole genome duplication event has occurred. The potential BIA biosynthetic pathway of *P. amurense* was proposed, and two PR10/Bet v1 members, 14 CYP450s, and 33 methyltransferases were selected as related to BIA biosynthesis. One PR10/Bet v1 was identified as norcoclaurine synthase, which could catalyze dopamine and 4-hydroxyphenylacetaldehyde into (*S*)-norcoclaurine.

Conclusion: Our studies provide important insights into the biosynthesis and evolution of BIAs in non-Ranunculales species.

1. Introduction

Benzylisoquinoline alkaloids (BIAs) are a diverse group of biologically active metabolites produced mainly in the species of early-diverging eudicots, the order Ranunculales. Many plant-derived BIAs, such as berberine, noscapine, morphine, and cepharanthine, have been widely used in the clinical treatment of tumors, analgesics, coronavirus, tuberculosis, diabetes, obesity, antidepressant, and hyperlipidemia (Ilyas et al., 2020; Imenshahidi & Hosseinzadeh, 2019; Liu, Meng, Wu, Qiu, & Luo, 2019; Ozturk et al., 2021; Wang et al., 2017; Yi, Zhu, Dong, Chen, & Li, 2021; Yin, Ye, & Jia, 2012). *Papaver somniferum* L. from Papaveraceae and *Coptis japonica* Makino from Ranunculaceae have long been used as the model plant species to study BIA biosynthesis and the whole biosynthetic pathway of some BIAs, especially berberine. For BIAs biosynthesis, first, dopamine and 4-hydroxyphenylacetaldehyde (4-HPAA) are condensed by norcoclaurine synthase (NCS) via Pictet-Spengler cyclization to form the BIA skeleton, (*S*)-norcoclaurine (Minami, Dubouzet, Iwasa, & Sato, 2007). (*S*)-norcoclaurine is further converted into the central intermediate (*S*)-reticuline by a sequence of reaction steps, including *O*-methylation (norcoclaurine-6-*O*-methyltransferase, 6-OMT) and *N*-methylation (coclaurine *N*-methyltransferase, NMT), cytochrome P450 (CYP450) (CYP80B2),

* Corresponding authors.
E-mail addresses: mawei@hljucm.edu.cn (W. Ma), zcxu@nefu.edu.cn (Z. Xu).
[1] These authors contributed equally to this work.

https://doi.org/10.1016/j.chmed.2024.11.003
1674-6384/

O-methylation again (3′-hydroxy-*N*-methylcoclaurine 4′-*O*-methyltransferase, 4′-OMT), and berberine bridge enzyme (BBE) catalysis. Finally, berberine is formed by a multi-step catalytic process involving scoulerine 9-*O*-methyltransferase (SMT), CYP719, and tetrahydroberberine oxidase (THBO, a flavin adenine dinucleotide-containing berberine bridge enzyme) (Sato, 2013; Yamada, Yoshimoto, Yoshida, & Sato, 2016). Comparative genomics from *C. japonica*, *Macleaya cordata* (Willd.) R. Br., *P. somniferum*, *Corydalis tomentella* Franch., and *Aquilegia coerulea* suggested that the *NCS*, *OMT*, *NMT*, *BBE*, and *CYP450* genes related to berberine biosynthesis are highly conserved in Ranunculales species. In fact, direct extraction of BIAs from plants is often impractical due to their low accumulation levels, making extraction process expensive and time-consuming (Ghirga et al., 2017). In recent years, chemical synthesis (Tajiri, Yamada, Hotsumi, Makabe, & Konno, 2021) and microbial fermentation engineering (Minami et al., 2008) were used to produce BIAs. However, it is difficult to cost-effective chemical synthesis due to their complex structures. Besides, metabolic engineering via microbe remains less efficient.

Phellodendron amurense Rupr., a deciduous tree in the family Rutaceae, has been used in traditional Chinese medicine for thousands of years (Dulan, Wang, Wu, Ling, & Anggelima, 2022; Xian et al., 2014). The species are distributed mainly in northeastern China, Korea, and Japan (Xian et al., 2014). The dried bark of *P. amurense* (Guanhuangbo) has been recorded in the *Chinese Pharmacopoeia* as an antiphlogistic, antibacterial, and anti-inflammatory agent for treating diarrhea, icterus, ulcer, carbuncle, and eczema (Chinese Pharmacopoeia and Commission, 2020; Dulan et al., 2022; Tang & Eisenbrand, 1992). Due to a drastic reduction in wild populations from long-term harvesting and habitat degradation, as well as its high economic and medicinal value, *P. amurense* was included on the list of vulnerable species and class II national protected plants in 1992 (Zhang et al., 2014). Interestingly, *Phellodendron,* from the order Sapindales (distantly related to Ranunculales), can largely accumulate BIAs, including BBE, columbamine, tetrahydropalmatine, and jatrorrhizine (Xian et al., 2014). Li et al. (2022) identified six candidate structural genes involved in the biosynthesis of BIAs in *P. amurense*, including *NCS*, glutamic-oxaloacetic transaminase 2 (*GOT2*), tyramine oxidase (*TYNA*), codeine-*O*-demethylase (*CODM*), tyrosinase (*TYR*), tyrosine aminotransferase (*TAT*), and protein *O*-mannosyltransferase 1 (*PSOMT1*), but the functions of these genes need further verification (Li et al., 2022). Additionally, CYP450 and methyltransferases as crucial genes of the BIAs biosynthesis pathway in *P. amurense* are still unknown. The biosynthetic pathway of BIAs in *P. amurense* is unclear and needs further research.

For the evolution of plant specialized compounds, the biosynthetic mechanism of identical secondary metabolites in distantly related species has been systematically studied. For instance, the mechanism of caffeine production in distant plants, including coffee, cacao, and tea, involves the tandem duplication of the *N*-methyltransferase (Denoeud et al., 2014). Concurrently, the functional convergence of nonhomologous gene families (CYP82 and CYP706) propels the biosynthesis of scutellarein in both *Scutellaria* and *Erigeron* (Gao et al., 2022). Here, the candidate genes involved in BIA biosynthesis from *P. amurense* were identified by combining transcriptome and metabolome analyses from multiple tissues. Interestingly, no homologous sequences corresponding to the reported BIA biosynthetic CYP80 and CYP719 were identified. Furthermore, the BIA biosynthesis pathway in *P. amurense* was proposed, and the norcoclaurine synthase activity of PR10/Bet v1 was verified. This research will provide insights into the evolutionary mechanism of plant specialized BIAs.

2. Materials and methods

2.1. Plant material and BIA standards

The *P. amurense* tissues were originally collected from *P. amurense* tree (7-year-old) grown in the Northeast Forestry University in Harbin, Heilongjiang Province, China (45°43′8″N, 126°37′35″E). As noted by Li et al. (2022), alkaloid production and distribution exhibit distinct organ and tissue specificity and vary at different stages of *P. amurense* stem development. To investigate this phenomenon, the eighteen representative tissues (Fig. 1A) were selected for testing, including phloem (R1) and xylem (R2) of secondary roots (lateral roots), and fibrous roots (absence of phellem) (R3), phloem and xylem of six different developmental stages stem (S1–S6-1/S1–S6-2) from a 2–3 year old branch, the phloem of the tree main trunk (B), petiole (P), leaf (L), and all the tissues were used for both RNA-seq and metabolomic analyses. Fresh tissue sample material was collected on June 26, 2022. All the samples were frozen in liquid nitrogen immediately after collection and stored at −80 °C until further analysis.

Authentic standards, including berberine (2086-83-1), coclaurine (2196-60-3), (*S*)-*N*-methylcoclaurine (3423-07-2), reticuline (485-19-8), scoulerine (6451-73-6), tetrahydrocolumbamine (483-34-1), palmatine (3486-67-7), magnoflorine (2141-09-5), jatrorrhizine (3621-38-3), rutaecarpine (20575-76-2), and phellodendrine (104112-82-5) were purchased from Chengdu Desite Biotechnology Co., Ltd. (Chengdu, China). (*S*)-Norcoclaurine (105990-27-0) and 4-HPAA (7339-87-9) were purchased from Toronto Research Chemicals (Toronto, Canada). Tyramine (51-67-2) was purchased from Shanghai Eon Chemical Technology Co., Ltd. (Shanghai, China). (*R*,*S*)-Norcoclaurine (5843-65-2) and dopamine (51-61-6) were purchased from Chengdu Push Biotechnology Co., Ltd. (Chengdu, China) and Macklin Inc. (Shanghai, China), respectively. The purities of these authentic standards were > 98%. Stock solutions of standards (1 mg/mL) were prepared in methanol, stored at −80 °C, and diluted in methanol to working solutions. Additionally, dopamine and 4-HPAA were prepared to concentrations of 2.5 mg/mL and 10 mg/mL in waters and methanol, respectively, stored at −80 °C. Liquid chromatography-mass spectrometry (LC-MS) grade methanol, acetic acid and acetonitrile were purchased from Thermo Fisher Scientific Inc. (Massachusetts, USA). Purified water was obtained from Watsons (Hong Kong, China). LC-MS grade ethanol and hexanes were acquired from Beijing Mreda Technology Co., Ltd. (Beijing, China).

2.2. Transcriptome sequencing and bioinformatic analysis

A total of 18 tissues of *P. amurense* were subjected to RNA-seq using an Illumina HiSeq Sequencing platform at the Pulang Ailui Biological Technology Co., Ltd. (Hangzhou, Zhejiang, China). Total RNA was extracted using the Plant RNA Purification Reagent (Trizol) (Invitrogen, USA) from each sample and RNA concentration and integrity were assessed based on the manufacturer's protocol. The raw data obtained by Illumina sequencing were first processed through Base Calling and converted into a FASTQ file format. Before assembly, the raw data were filtered using trimmomatic (version 0.39) software with default parameters to remove adapters and low-quality bases to obtain high-quality clean data (Bolger, Lohse, & Usadel, 2014). Clean data from different tissues were *de novo* assembled using TRINITY (version 2.13.2) with default settings (Grabherr et al., 2011). Furthermore, the redundant transcripts were removed to harvest the final unigenes. Subsequently, structural annotation and open reading frame (ORF) prediction of unigenes were performed using Trans-

decoder (version 5.5.0). The assembly completeness was further evaluated using Benchmarking Universal Single-Copy Orthologs (BUSCO) (version 5.2.2) (Manni, Berkeley, Seppey, Simão, & Zdobnov, 2021).

Unigenes were further annotated based on the following databases: Eukaryotic Orthologous Groups of proteins database (COG), Gene Ontology (GO), Kyoto Encyclopedia of Genes and Genomes (KEGG), NCBI nonredundant protein sequences (Nr), SwissProt, and Pfam protein families database (PFAM) with the Basic Local Alignment Search Tool (BLAST) *E*-value less than 1×10^{-5}.

The fragments per kilobase of transcript per million (FPKM) value from different tissues was calculated using bowtie2 (version 2.4.5). The RNA transcripts with adjusted $\log_2FC \geq 2$ and adjusted $P < 0.001$ were assigned as differentially expressed genes (DEGs). Synonymous substitutions per synonymous site (K_S) distributions of paralogous genes were calculated to detect the whole-genome duplication (WGD) event in *P. amurense* using wgd pipeline (Yang, Li, Chen, Sun, & Lu, 2019).

2.3. Targeted metabolome analysis

These 18 tissue samples, with three biological replicates of each sample, were used to extract metabolites for the relative quantitative analysis of alkaloids. All the samples were dried, crushed, and sieved through a No. 50 mesh sieve. Approximately 20 mg of the sieved powder was weighed and mixed with 2.0 mL of 70% methanol under vortex for 1 min, followed by ultrasonic extraction at 100 kHz for 45 min, centrifuged at 12 000 r/min for 10 min, and the supernatant was filtered through a 0.22 μm membrane.

Metabolites were identified and quantified using the Agilent UPLC 1290 system combined with a G6500 quadrupole time-of-flight mass spectrometer (QTOF) and G6400 triple quadrupole mass spectrometer (QQQ) (Agilent Technologies, Santa Clara, CA, USA) following the reported method (Yang et al., 2020). Both QTOF and QQQ use an electrospray ionization (ESI) source. Metabolites were identified using retention time and mass spectra of the positive and negative ion modes of QTOF and annotating against public databases, including MassBank (https://www.massbank.jp/), ReSpect (https://spectra.psc.riken.jp/), mzCloud (https://www.mzcloud.org/), KNAPSAcK (https://kanaya.naist.jp/KNApSAcK/), and HMDB (https://www. hmdb.ca/). The operating parameters of QTOF were set as follows: sheath gas temperature 350 °C, sheath gas flow 11 L/min, gas temperature 320 °C, gas flow 10 L/min, nebulizer 206 kPa, capillary voltage 4 000 V, fragmentor 120 V, collision energies 30 V.

We quantified metabolites using multiple-reaction monitoring (MRM) of QQQ in the positive ion ($[M + H]^+$) modes. The operating parameters of QQQ were set as follows: sheath gas temperature 250 °C, sheath gas flow 11 L/min, gas temperature 300 °C, gas flow 5 L/min, nebulizer pressure 310 kPa, capillary voltage 3 500 V, fragmentor 120 V. The optimized collision energies (CE) were described in Table S1. After data acquisition finished, we extracted LC-MS data of qualitative compounds using Qualitative Analysis 10.0 and corrected the peak area by manual integration. Before principal component analysis (PCA) and heatmap analysis, the corrected data were normalized by the standardization method.

The MS scan functions and the UPLC solvent gradients were controlled using Agilent MassHunter Workstation Software. The analytical conditions were set as follows: Agilent Eclipse Plus C_{18} column (100 mm × 2.1 mm, 1.8 μm), injection volume: 3 μL, temperature: 35 °C, flow rate: 0.3 mL/min, detection wavelength: 210 nm and 245 nm, solvent system: water containing 0.1% formic acid (A) and acetonitrile (B), and gradient program: 95% A (0–2 min), 95%–75% A (2–4 min), 75%–70% A (4–9 min), 70%–40% A (9–19 min), 40%–10% A (19–25 min), 90%–100% B (25.1–27 min), 0–95% A (27–32 min), and 95% A (32–34 min).

To obtain data that could be evaluated for repeatability, 10 μL solution from each stock solution of standards were mixed and used as quality control (QC) samples. The QC sample was injected at regular intervals (every 10 samples) throughout the analysis.

2.4. Weighted gene co-expression network analysis (WGCNA)

WGCNA was performed to assess the gene co-expression networks associated with berberine content in *P. amurense* using the WGCNA R package (version 1.70.3) (Langfelder & Horvath, 2008). All coding genes were used for WGCNA with the following settings: $\log_2FC > 1$, CPM values >1, minimum module size of 150, and minimum height for merging modules of 0.25. Moreover, the genes from concerned modules related to berberine accumulation were extracted, enriched, and annotated using the GO and KEGG databases.

2.5. Identification of candidate genes in protoberberine alkaloid pathway

The reported seed genes related to BIA biosynthesis in Ranunculales species, including *CjPR10A* (*C. japonica* PR10A, BAF45338.2) *PsNCS2* (*P. somniferum* NCS2, AAX56304.1) (Liscombe, MacLeod, Loukanina, Nandi, & Facchini, 2005; Minami et al., 2007), *Cj6OMT* (*C. japonica* norcoclaurine 6OMT, Q9LEL6.1), *Cj4′OMT* (*C. japonica* 3′-hydroxy-*N*-methylcoclaurine 4′OMT, Q9LEL5.1), *CjSOMT* (*C. japonica* scoulerine 9OMT, Q39522.1) (Morishige, Tsujita, Yamada, & Sato, 2000), *CNMT* (Q948P7) (Choi, Morishige, Shitan, Yazaki, & Sato, 2002), *PsCYP80B1* (*P. somniferum* CYP80B1, AAF61400.1) (Huang & Kutchan, 2000), *CjCYP80B2* (*C. japonica* CYP80B2, BAB12433.1) (Ikezawa et al., 2003; Luo et al., 2010), *CjCYP719A1* (*C. japonica* CYP719A1, BAB68769.1) (Ikezawa et al., 2003), *PsCYP719B1* (*P. somniferum* CYP719B1, ABR14720.1) (Gesell et al., 2009), and internal reference genes (18S-RNA, XP_026401101.1; RubisCo, XP_026449780.1) (Guo et al., 2018) were downloaded from National Center for Biotechnology Information (NCBI). The homologous of seed genes were identified using BLASTP (version 2.2.31) with an *E*-value of less than 10^{-5}. The identification of CYP450 members referred to the CYP nomenclature system: CYP450s with more than 40% identity were grouped into the same family, and CYP450s with more than 50% identity were grouped into one subfamily.

Multiple sequence alignments for candidate genes were performed using MAFFT (version 7.490) (Katoh, Misawa, Kuma, & Miyata, 2002). TrimAL (version 1.4.1) was used to trim the sequence and remove the gap, and IQ-TREE (version 2.1.4) was used to construct phylogenetic trees of candidate genes in the 1000 times bootstrap (Capella-Gutiérrez, Silla-Martínez, & Gabaldón, 2009). Finally, the optimal alternative models of phylogenetic analysis for alignments were selected using an automated selection of parameters.

2.6. Cloning, protein expression and enzyme assays of PaNCS1 gene

To evaluate the catalytic activity, the open reading frames of *PaNCS1* was obtained and cloned into the pMAL-2CX vector. Recombinant plasmids of *PaNCS1* gene expressed in *Escherichia coli* BL21 (DE3) (Tsingke Biotechnology, Hubei, China). *E. coli* cells containing each recombinant plasmid were grown at 37 °C in Luria Bertani (LB) medium with 50 μg/mL kanamycin and induced with 0.3 mmol/L isopropyl-*β*-*D*-thiogalactoside (IPTG) at 16 °C, cells containing recombinant plasmid were incubated at 130 r/min in shaker for 24 h, respectively. The cells were collected by centrifu-

gation (5 000 r/min for 10 min at 4 °C) and resuspended in buffer (50 mmol/L Tris-HCl pH 7.4, 5 mmol/L β-mercaptoethanol, 10% glycerine). After sonication, the sample was centrifuged at 12 000 r/min for 15 min at 4 °C, and the supernatant was collected as crude enzyme preparation. Subsequently, Dextrin Beads Gravity Column Kit (Smart-Lifesciences Biotechnology Co., Ltd., Changzhou, China) was used for protein purification, following the provided instructions. These purified proteins were then analysed using sodium dodecyl sulphate-polyacrylamide gel electrophoresis (SDS-PAGE) (Sparkjade, Shangdong, China).

The enzyme activity of *PaNCS1* gene was determined in buffer (50 mmol/L Tris-HCl pH 7.4, 5 mmol/L β-mercaptoethanol, 10% glycerine) (70 μL) containing substrates 40 μL dopamine (2.5 mg/mL), 10 μL 4-HPAA (10 mg/mL) and 80 μL enzyme. After incubation at 37 °C for the night, reactions were stopped by adding 1/2 vol of methanol. The reaction products were centrifuged at 12 000 r/min for 15 min and the supernatant was detected by Agilent UPLC 1290 system combined with a G6400 triple quadrupole mass spectrometer (QQQ) (Agilent Technologies, Santa Clara, CA, USA). The analytical conditions were set as follows: Ultimate Cellu-J (150 mm × 4.6 mm, 5 μm), temperature: 30 °C, flow rate: 0.8 mL/min. The solvent system consisted of ethanol (A) and hexanes (B), and isometric program: 30% A (0–20 min).

3. Results

3.1. Transcriptome analysis of different tissues of P. amurense

RNA sequencing of 18 different tissues produced 682 766 942 raw reads, and 682 057 543 clean reads were obtained after filtering reads with low-quality and adapters. The average guanine-cytosine (GC) content was 47.29%, ranging from 45.36% to 51.6% (Table S2). A total of 109 673 unigenes were *de novo* assembled and filtered with an average length of 818 bp and an N50 length of 1 122 bp. The complete estimation of transcriptome assembly showed that 74.7% of Embryophyta BUSCO gene sets were identified as "complete". Results of functional annotation showed that 58 204 (53.1%), 37 665 (34.3%), 56 236 (51.3%), 62 186 (56.7%), 48 603 (44.3%), and 39 226 (35.8%) unigenes were annotated against databases of COG, GO, PFAM, Nr, SwissProt, and KEGG,

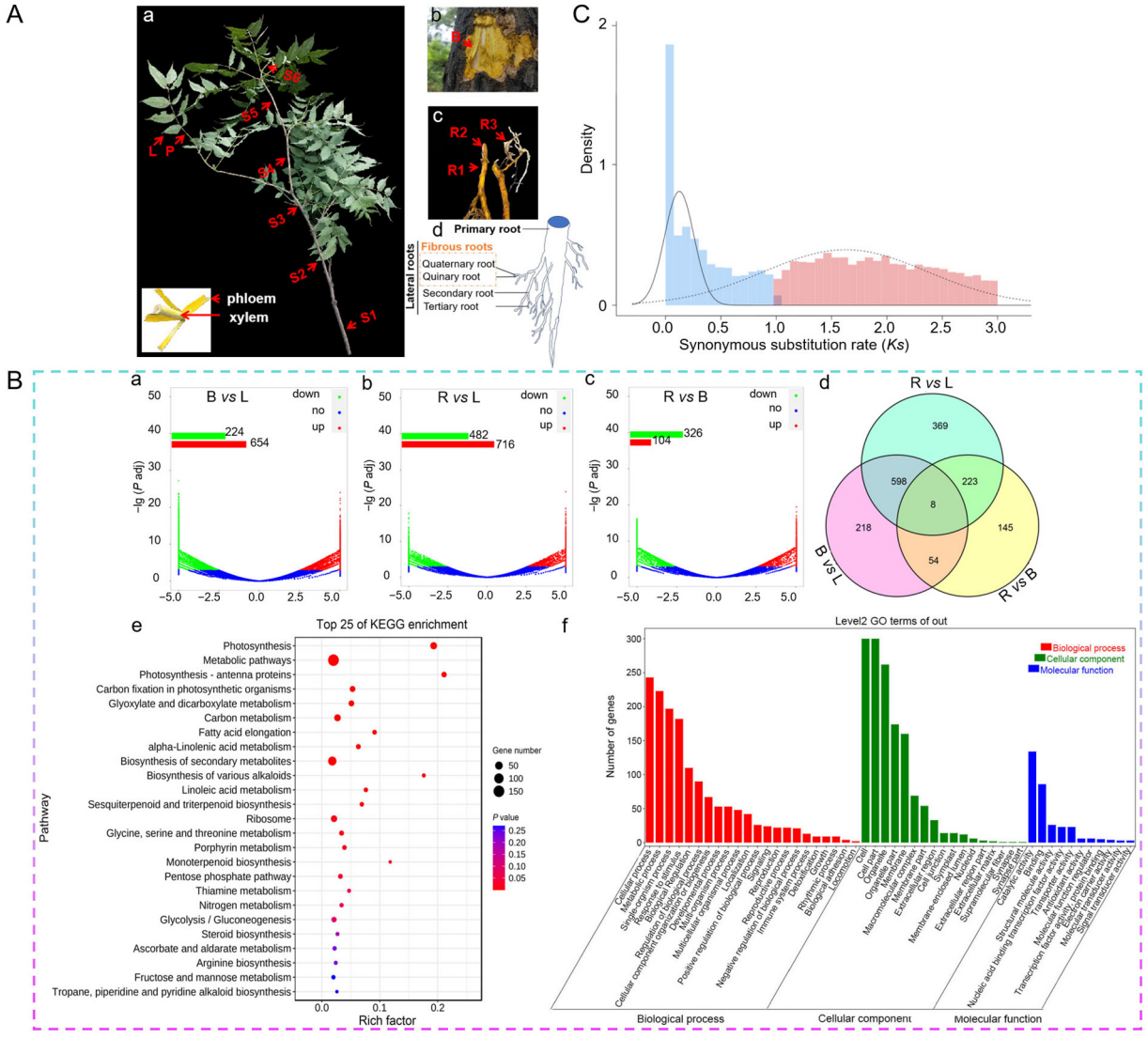

Fig. 1. Transcriptome analysis of *P. amurense*. (A) Sampling diagram of *P. amurense*, (a) different developmental stages of stem (S1–S6, "-1" for phloem, "-2" for xylem), petiole (P), and leaf (L); (b) phloem of tree main trunk (B); (c) phloem, xylem, and fibrous of roots (R1/R2/R3); (d) illustration of root tissue. (B) Identification and enrichment analysis of DEGs for the R *vs* L, R *vs* B and B *vs* L groups, (a–c) Volcano maps; (d) Venn diagrams; (e) KEGG and (f) GO enrichment analyses of DEGs in characteristic parts (roots, leaves, and barks). (C) Transcriptome-based analysis of WGD events.

respectively (Table S3). Here, 65 153 coding genes from *P. amurense* unigenes were identified, of which 40 203 were paralogous gene pairs. The distributions of K_S for all paralogous genes showed a clear peak at $K_S \approx 0.32$, suggesting that at least once recent WGD event occurred after speciation (Fig. 1C).

To identify genes associated with berberine accumulation in *P. amurense*, representative parts with significant differences in berberine content, such as R (R1) (high content), B (high content), and L (low content), were selected for DEG analysis. A total of 2,506 candidate DEGs were identified from R, B, and L. Volcano plots (Fig. 1B, a–c) showed 1 198 (716 genes up-regulated and 482 genes down-regulated), 878 (654 genes up-regulated and 224 genes down-regulated), and 430 (104 genes up-regulated and 326 genes down-regulated) DEGs in R *vs* L, B *vs* L, and R *vs* B, respectively. The venn diagram (Fig. 1B, d) showed DEGs overlap between the three tissues across compared groups. The R *vs* L had 598 identical DEGs to the B *vs* L, suggesting that these DEGs may be associated with differences in berberine accumulation. Subsequently, functional enrichment of DEGs indicated that 70 DEGs were enriched in the "biosynthesis of secondary metabolites", such as terpenoids, flavonoids, and steroids (Fig. 1B, e–f). However, we could not annotate the BIA biosynthetic pathway via KEGG enrichment. We then performed DEGs analysis on the phloem of the stem at different developmental stages (S6-1 to S1-1) and obtained a total of 765 DEGs, which contained only one gene (*TRINITY_DN515_c0_g1_i4*) annotated to the "isoquinoline alkaloid biosynthesis" (ko00950) (Fig. S1). These results suggest that the biosynthesis of BIAs in *P. amurense* might be a distant relative of the reported BIA biosynthetic pathway from Ranunculales species.

3.2. Targeted metabolomic profiling in P. amurense

A total of 28 metabolites, including dopamine, tyramine, and 26 BIAs, were successfully characterized using ultra-performance liquid chromatography coupled with quadrupole/time-of-flight mass spectrometry (UPLC-QTOF-MS) (Table S1). Ultra-high-performance liquid chromatography coupled with triple quadrupole mass spectrometry (UPLC-QQQ-MS) further optimized the collision energy (CE) of these 28 components (Fig. S2A). Subsequently, the relative content levels of the 28 compounds in the 18 tissues of *P. amurense* were quantified based on the peak areas with the MRM mode (Table S4). A principal component analysis (PCA) (Fig. S2B) showed the steady and reliability of the metabonomic test. The heatmap of hierarchical clustering also showed that the biological replicates were grouped based on the content levels of the compounds. Besides, the accumulation of different BIA compounds in different tissues of *P. amurense* varied considerably (Fig. 2A). Phenotypic observations revealed that both phloem and xylem were transformed from green to yellow during stem development, and the colour of phloem was always deeper (Li et al., 2022). The content of berberine in the phloem was always higher than xylem during S1–S6. Noteworthy, there was no significant difference in the content of berberine between the phloem of the S3–S1 developmental stages, indicating that berberine would not accumulate with time after reaching a certain level (Fig. 2B). While norcoclaurine, dopamine and reticuline were higher in S6, S5, and S4 than in S3, S2, and S1 (Fig. 2A). The contents of protoberberine alkaloids, including berberine, oxyberberine, jatrorrhizine, 8-oxoepiberberine, columbamine, phellodendrine, tetrahydrojatrorrhizine, 8-oxypalmatine, and palmatine, are highly accumulated in the roots and bark of *P. amurense* (Fig. 2A), which is consistent with previous reports (Zhang et al., 2014). Some alkaloids were also specifically highly accumulated in leaves and petioles, including tetrahydropalmatine and rutaecarpine.

3.3. Selection of candidate BIA biosynthetic genes using WGCNA

To elucidate berberine biosynthesis in *P. amurense*, WGCNA, integrating transcriptome and metabolome from multiple tissues, was employed, identifying the correlation between BIA accumulation and transcript expression profiles. The WGCNA clustering indicated that all transcripts were grouped into 24 unique modules in *P. amurense* (Fig. 3A). The MEturquoise module contained the most genes (32,229 genes), whereas the MEdarkgreen module had the fewest genes (224 genes). Pearson's correlation analysis ($r > 0.8$) between transcript expression and BIA accumulation showed that 1 799 transcripts in the MEblack module was significantly positively correlated with the content of protoberberine alkaloids, including berberine, jatrorrhizine, columbamine, phellodendrine, and oxyberberine. The other protoberberine alkaloids, such as 8-oxoepiberberine, palmatine, and 8-oxypalmatine, were positively associated with the MEpink (1,735 transcripts) module. Also, the intermediate norcoclaurine and reticuline were positively correlated with the MEyellow (2 010 transcripts) module. Additionally, some BIAs were positively associated with the MEcyan (884 transcripts) and MEmidnightblue (749 transcripts) modules.

KEGG enrichment analysis showed that two genes (*PaTyrAT1* and *PaTyrAT2*) associated with the isoquinoline alkaloid biosynthesis pathway (K14455 and K14454) were detected in MEblack module (Table S5). The gene structure and phylogeny (Fig. S3) indicated that these two genes belonged to the pyridoxal 5′-phosphate (PLP)-dependent aminotransferase family, encoding tyrosine aminotransferase (TyrAT), and were responsible for forming tyramine and 4-HPAA. Moreover, *TyrAT2* was high expression in the root, bark, and phloem (Fig. 3C), consistent with the enrichment trend of berberine (Fig. 2B), indicating this gene may be related to berberine biosynthesis. However, the genes from co-expression modules could not be mapped into the downstream biosynthetic pathway of BIAs, suggesting that the BIA biosynthesis of *P. amurense* might have evolved independently with the reported biosynthetic pathway of Ranunculales species.

A total of 49 candidate genes were identified from MEblack, MEcyan, MEpink, MEmidnightblue, and MEyellow, including 14 *CYP450s*, two *NCSs*, and 33 *MTs*. These genes showed a similar trend as berberine enrichment (Fig. 3C). Although substantial biochemical evidences are still needed, based on the above findings and regarding berberine biosynthetic pathways in other plants, a potential berberine synthesis pathway in *P. amurense* was proposed (Fig. 3B).

3.4. Phylogenetic analyses of PaMTs and PaCYP450s

The chemical composition and structure of BIAs implied that the CYP450s played a crucial role in modifying the structural diversity of BIAs, including hydroxylation, C–C phenol-coupling, and C–O phenol-coupling action of BIAs in *P. amurense*. Here, a total of 95 CYP450s and 68 MTs were identified from the remaining modules in *P. amurense*. Interestingly, the sequence identity between *P. amurense* CYP450s and reported BIA biosynthetic CYP80 and CYP719 was less than 40%; however, the similarity of internal reference genes was more than 49% (Table S6), indicating there were no CYP80 and CYP719 families in *P. amurense*. Further phylogenetic analysis showed that 11 out of 14 CYP450 candidate genes were clustered in 71 clan, including CYP76, 706, 71, 83, 79, and 89 families, the largest CYP clan conserved in the land plants (Fig. 4). The remaining three genes were clustered in 72 clan (CYP72), 85 clan (CYP88), and 86 clan (CYP94).

MTs also played an essential role in the diversification of BIAs, including *O*- and *N*-MTs. The reported MTs can be phylogenetically divided into diverse branches, including 6-OMT, 4′-OMT, SMT, and

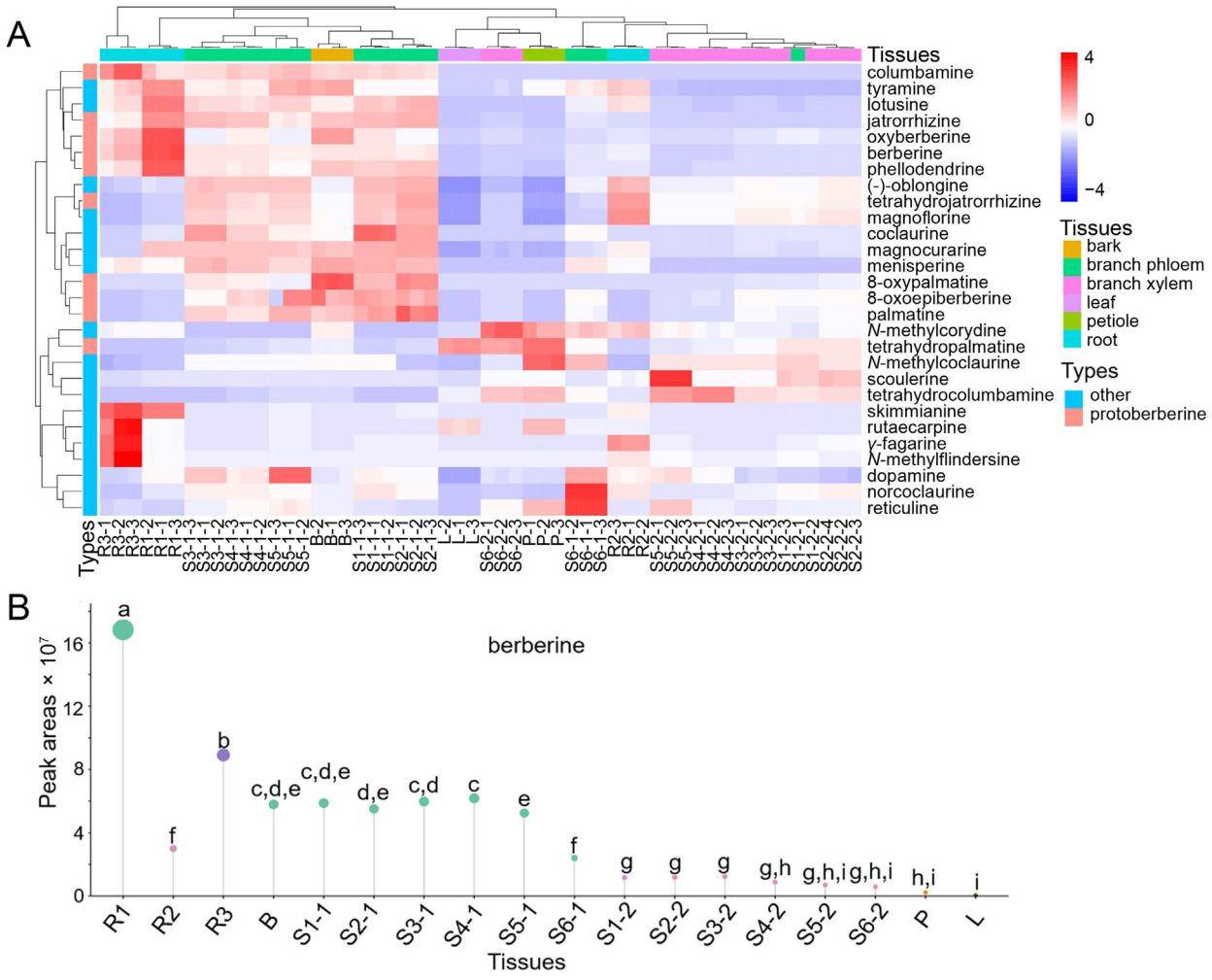

Fig. 2. Targeted metabolomics analysis of *P. amurense*. (A) Heatmap based on hierarchical clustering analysis. (B) Content change of berberine in *P. amurense*. *X*-axis is different tissues of *P. amurense*, and *Y*-axis is peak area of berberine in corresponding tissues detected by LC-MS. The "a-f" designation represents the differences between various tissues. When letters are identical, it signifies that there is no difference between two comparison groups. The greater the number of differing letters between comparison groups, the more significant the difference between the two tissues.

NMT (Dang & Facchini, 2012). A total of 33 MT candidate genes, including two NMT and 31 OMT genes, were identified by WGCNA (Table S7). Out of 31 OMTs, 24 were clustered with SMTs from *C. sinensis*, *C. japonica, C. chinensis,* and *P. amurense* and the rest were clustered with OMT as a branch (Fig. S4). Notably, the candidate MTs in *P. amurense* were distantly related to homologous genes in the Ranunculales. Specifically, 58 out of 68 MTs in *P. amurense* have less than 50% similarity to the reported BIA biosynthetic MTs in *C. japonica* (Table S6).

3.5. Functional identification of PR10/Bet v1 related to NCS

(*S*)-Norcoclaurine is the central intermediate metabolite of berberine biosynthesis, which is synthesized from dopamine and 4-HPAA by the catalytic activity of NCS, a member of the PR10/Bet v1 family. NCS can be subdivided into two subfamilies, NCSI and NCSII clades, and only the genes from the NCSI clade can form (*S*)-norcoclaurine (Vimolmangkang et al., 2016). Here, two NCS transcripts from *P. amurense* were identified (Table S7), and *PaNCS1* was clustered in the NCSI clade (Fig. 5A). Furthermore, multiple sequence alignment analysis revealed the *PaNCS1* contained the NCS active sites formed by side chains of tyrosine, lysine, aspartic acid, and the ligand-binding domain (glycine-rich loop) of the Bet v1 protein family (Ilari et al., 2009) (Fig. 5B). The gene expression of NCS transcripts showed that the *PaNCS1* gene was lower in the shoots (S4–S6) than the older branches (S1–S3), both in the phloem and xylem. The *PaNCS2*, however, showed no significant expression trend in different tissues (Fig. 3C). Subsequently, recombinant protein of *PaNCS1* was used to validate the catalytic activity of NCSs. The results showed that a new peak was generated under the catalysis of *PaNCS1* using dopamine and 4-HPAA as substrates, and the product is identical with the standard of (*S*)-norcoclaurine and (*R, S*)-norcoclaurine (Fig. 5C, Fig. S5). The result demonstrated that *PaNCS1* could perform the catalytic activity of NCS, which could condense the dopamine and 4-HPAA to form (*S*)-norcoclaurine.

4. Discussion

BIAs, as a class of secondary metabolites in medicinal plants, exhibit diverse pharmacological activities and play pivotal roles in plant growth and survival by conferring protection against external biotic and abiotic stresses, and reducing competition for nutrients from neighboring plants (Wink, 2015). Particularly, berberine, as a vital BIA, has been traditionally used to treat various diseases (Habtemariam, 2016; Yi et al., 2021; Jain, Tripathi, & Tripathi, 2023). Besides, it is used in agricultural fields as an insecticide (Miyazawa, Fujioka, & Ishikawa, 2002), herbicide (Iwasa,

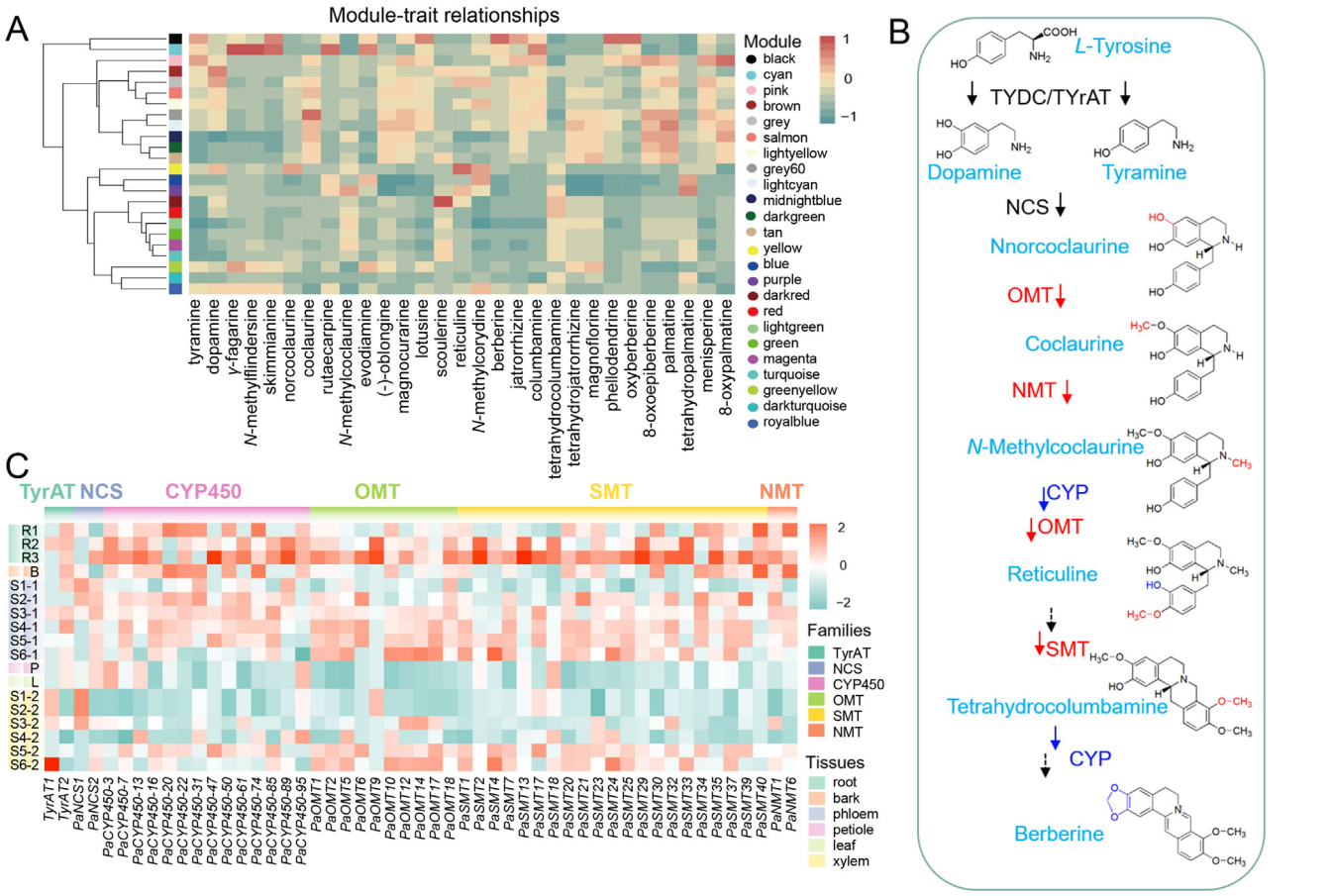

Fig. 3. WGCNA of metabolites and transcriptomics based on all 18 tissues of *P. amurense*. (A) Correlation heatmap between alkaloids (bottom) and 24 gene modules (left). "Modules" are clusters of highly interconnected genes. In an unsigned coexpression network, modules correspond to clusters of genes with high absolute correlations. Red and greener represent positive and negative correlations, respectively. (B) A proposed berberine biosynthetic pathway in *P. amurense*. The fan diagram next to structural formula shows relative contents of corresponding compounds in 18 different tissues of *P. amurense*, with green to red indicating low to high compound content, where darker red indicates higher compound content. (C) Heatmap analysis of relative expression of candidate genes in different tissues based on FPKM values. The colors reflect relative expression levels of genes in different tissues, with darker red indicating higher relative gene expression levels and darker green indicating lower relative gene expression levels.

Moriyasu, & Nader, 2000), and to control bacterial wilt disease in tomato plants (Liang et al., 2022), and increase resistance against tobacco mosaic virus in tobacco (Guo et al., 2020). *P. amurense* is known for its high BIA content, particularly the protopine and berberine alkaloids. The distribution and concentration of these alkaloids have been shown to differ significantly across various tissues of *P. amurense*, as well as throughout different developmental stages of the same tissue (Li et al., 2022; Zhang et al., 2014). The distribution and accumulation mechanisms of BIAs in *P. amurense* remain unclear. Our study reveals that most protoberberine-type alkaloids accumulate heavily in the root and phloem, but not in the xylem, petiole, or leaf. Interestingly, some alkaloids, such as tetrahydropalmatine and rutaecarpine, show the opposite trend, being more abundant in the leaves and petioles of *P. amurense*. Thus, utilizing the leaves of *P. amurense* may be an efficient approach to avoid wasting valuable resources. Another recent study on *P. amurense* stem development has shown that berberine accumulates with the progression of stem development, which our study confirms (Li et al., 2022). However, we also observe that berberine no longer accumulates after reaching a certain developmental stage, possibly due to substrate consumption, including norcoclaurine, dopamine, and reticuline.

For BIAs production, microbial fermentation offers a sustainable and environmentally friendly alternative with shorter production cycles and higher yields (Cao, Gao, Suástegui, Mei, & Shao, 2020). However, reconstituting plant-derived BIA biosynthesis in microbial hosts has been challenging, as some of the enzymes involved are unsuitable for heterologous expression. Currently, our understanding of BIA biosynthetic pathways is limited to model plants such as *C. japonica* and *P. somniferum*. Recent advances in next-generation sequencing data have enabled a more in-depth elucidation of some biosynthetic pathways. Transcriptome and metabolome association analysis can identify candidate genes with potential roles in biosynthetic pathways. Microbial systems incorporating plant genes enable the mass production of scarce BIAs (Minami et al., 2008). Thus, studying the berberine synthesis pathways in *P. amurense* and identifying more functional genes are crucial for generating BIAs using microbial fermentation technology.

Despite their complex and diverse structures, BIAs share a common biosynthetic precursor, (*S*)-norcoclaurine, which is formed by the condensation of dopamine and 4-HPAA catalyzed by NCS. The introduction of a chiral center by NCS is considered essential for all stereoselective enzymatic reactions in the BIA biosynthetic pathway (Ghirga et al., 2017). NCS has been extensively studied in *P. somniferum* and related species, and has been successfully heterologously identified in *E. coli* (Pasquo et al., 2008; Samanani & Facchini, 2001; Samanani, Liscombe, & Facchini, 2004). Here, NCS activity in *P. amurense* was identified and confirmed via expressing NCS recombinant proteins in *E. coli*, suggesting that NCS activity is relatively conserved across species.

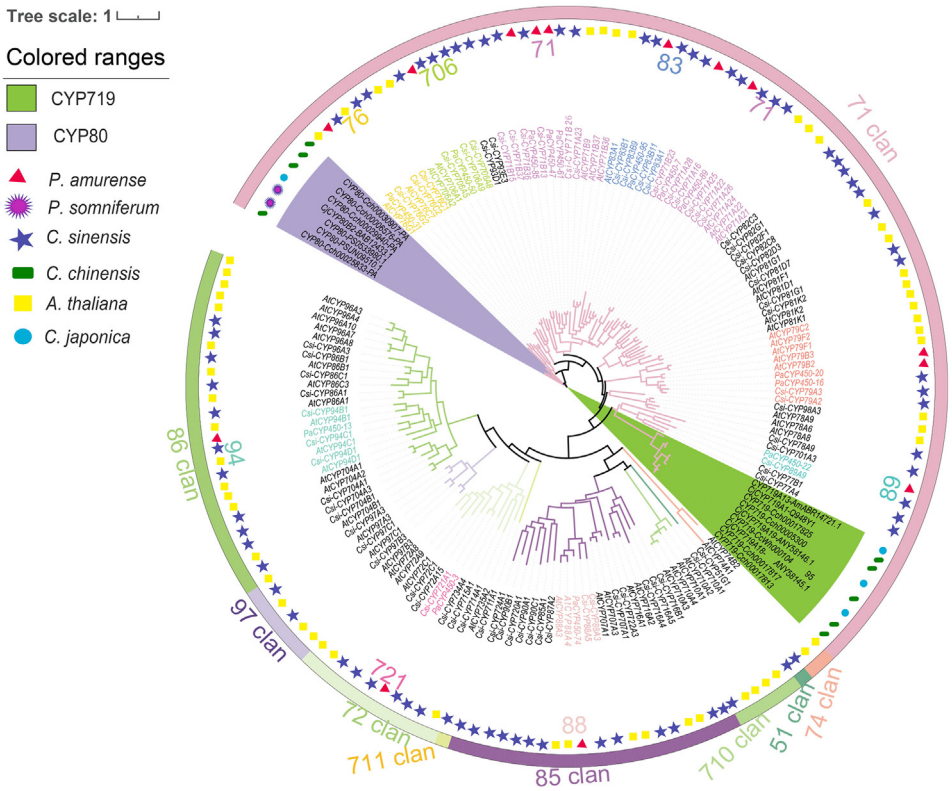

Fig. 4. Independent evolution of berberine biosynthesis between *P. amurense* and Ranunculales species. A phylogenetic tree was constructed by combining 14 candidate CYP450s in *P. amurense* with CYP450s in *A. thaliana*, *C. sinensis*, *C. japonica*, *C. chinensis*, and *P. somniferum*. The ML phylogenetic tree was constructed using iqtree with a bootstrap test (replicated 1 000 times).

An interesting phenomenon is that berberine can accumulate in many eudicot plants, including in distant species *P. amurense* and *C. japonica* (Chi, Van Hung, Le Thanh, & Phi, 2020). Indeed, it is common in nature for distantly related species to produce the same secondary metabolites. Conventional studies on berberine in *P. amurense* have focused primarily on extraction (Wang, Li, Liu, & Chen, 2015), isolation, purification, structure identification (Xian et al., 2014), and activity (antioxidant, antimicrobial, and anti-Herpes simplex virus type 1 activity) (Wang et al., 2009). Although these studies help identify the pharmacologically active components, there was little information on the berberine accumulation mechanism in *P. amurense*. Based on the WGCNA results, this study suggests a novel evolutionary may occurrence in berberine production within *P. amurense*.

Several studies have shown that gene expansion may shape the evolution of quality and secondary plant metabolite biosynthesis, for example, the capsaicinoid biosynthesis in hot pepper (Kim et al., 2014) and the special flavor and appearance of *Zanthoxylum bungeanum* Maxim. (Feng et al., 2021). The WGD event has dominated the evolutionary history of plants (Van de Peer, Mizrachi, & Marchal, 2017; Wendel, 2015). Consistent with this statement, we suggest that a recent WGD event ($K_S \approx 0.32$) may have shaped the evolution of BIAs biosynthesis, especially berberine, in *P. amurense*. The K_S peak value was less than the K_S distribution of ancient gamma hexaploidy shared among the core eudicots, and the close *Citrus* species have not undergone extra WGD event after gamma duplication event (Feng et al., 2021). Therefore, the WGD of *P. amurense* might be species-specific after the divergence from the genus *Citrus*. It is believed that the WGD event in *P. amurense* helps to distinguish the compounds of *P. amurense* from its close relative, *Citrus*.

Berberine biosynthesis largely depends on the expression of two CYP450s, methylenedioxy-bridge formation (catalyzed by CYP719 subfamily members) and hydroxylation (catalyzed by CYP80 subfamily members) (Mizutani & Sato, 2011; Pauli & Kutchan, 1998). Notably, CYP719 and CYP80B members have been identified as Ranunculales-specific (Nelson, Ming, Alam, & Schuler, 2008), although they are also present in the Magnoliales (Cui et al., 2022; Deng et al., 2018). Besides, multi-steps in berberine biosynthesis are mediated by a series of MTs. Here, some new candidate CYP450s and MTs were identified by WGCNA. Nevertheless, PaCYP450s share only 31.22% amino acid sequence identity with *C. japonica* counterparts, a similarity that could be expected from any two functionally unrelated random plant CYP450 enzymes, suggesting that the similar catalytic activities of CYP450s in the two lineages were derived from convergent evolution (Weng et al., 2010). In addition, the closely related *Citrus* did not accumulate BIA compounds and no homologs of CYP80 and CYP719. These results showed that the biosynthetic pathway of BIAs in *P. amurense* likely evolved independently after the split from Ranunculales and *Citrus*. According to previous reports, the CYP719 and the CYP80 families were possibly derived from CYP701 and CYP76 in the CYP71 clan, indicating that the genes clustered in the CYP71 clan might perform similar catalysis as in CYP719 and CYP80 families (Nelson et al., 2008). Collectively, a potential convergent or parallel evolution of berberine in *P. amurense* was proposed, although upstream of the synthesis was relatively conservative.

Identifying the new CYP450s and MTs in *P. amurense* will provide insight into the evolution of BIA biosynthesis. The present study identified 51 candidate enzyme genes in the BIA biosynthetic pathway and one of them was confirmed to have NCS catalytic activity. The expression levels of certain candidate genes exhibit

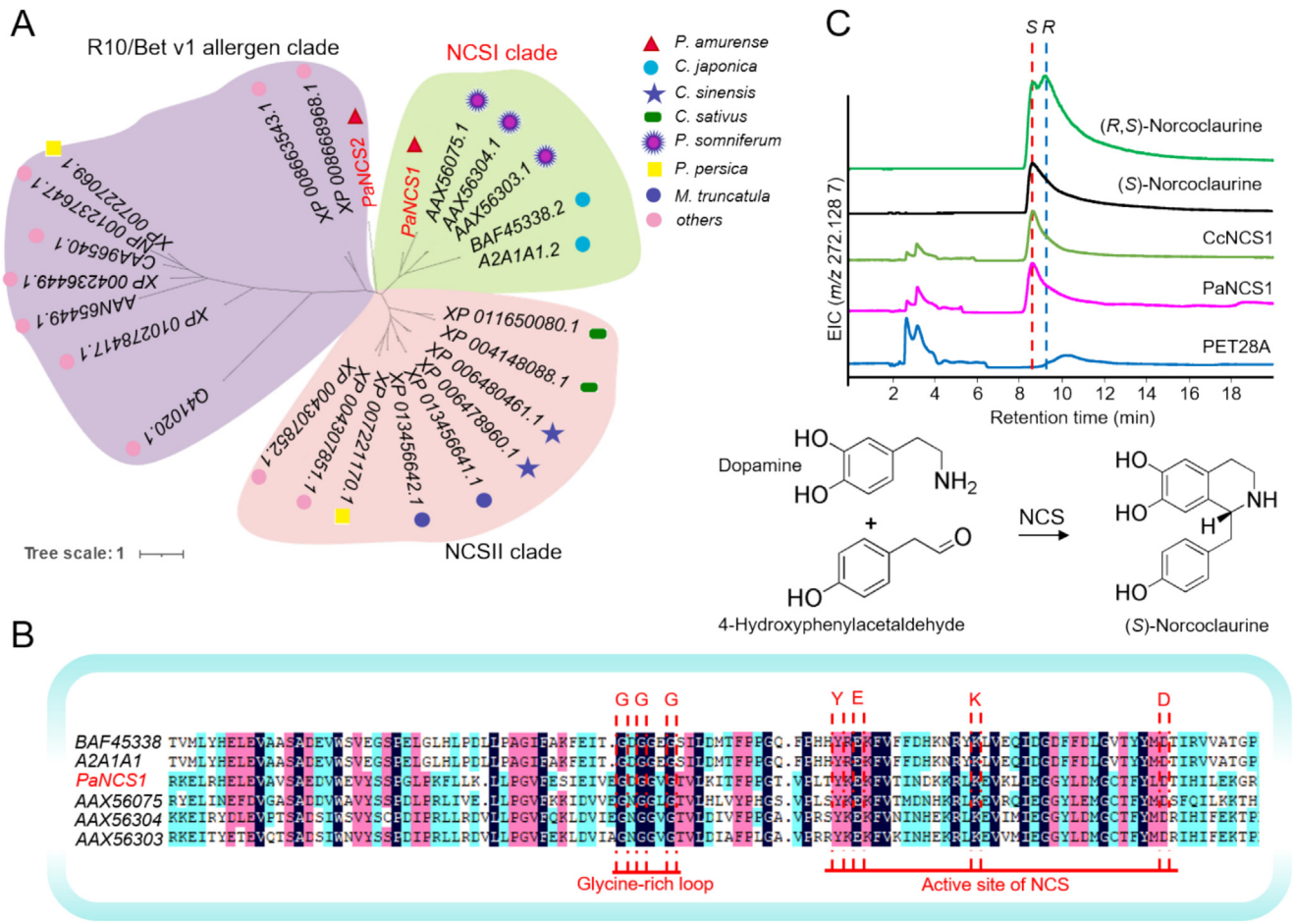

Fig. 5. Enzyme activity of NCSs in *P. amurense* analysis. (A) Phylogenetic tree of NCSs was constructed using iqtree with the bootstrap value of 1 000. ML phylogenetic tree analysed relationships of *NCSs* genes in *P. amurense*, *C. japonica*, *C. sinensis*, *P. somniferum*, and others. (B) Multiple sequence alignment was conducted between *PaNCS1* and homologous genes in *C. japonica* and Papaveraceae. (C) HPLC analysis of products from incubation of recombinant PaNCS protein with substrates dopamine and 4-HPAA. Authentic (*R*,*S*)-norcoclaurine and (*S*)-norcoclaurine were used for retention time comparison. *C. chinensis* NCS1 was used as a positive control for enzyme-catalyzed reaction. Spontaneous, non-enzymatic condensation was detected using PET28A as a negative control.

a positive correlation with the content of BIAs, particularly in the roots and bark, as compared to the leaves and petioles. Throughout various developmental stages of the stem, both BIAs and candidate genes are more abundant in the phloem. Nonetheless, some candidate genes show a weak correlation with catalytic product contents. For example, *NCS1* demonstrates an inverse relationship with (*S*)-norcoclaurine content changes during stem development. This phenomenon can be attributed to the fact that NCSs are considered enzymes that catalyze the Pictet-Spengler reaction (Sheng & Himo, 2019), which can synthesize (*S*)-norcoclaurine and tetrahydroisoquinoline by condensing dopamine with other aldehydes (e.g. benzaldehyde and cyclohexanecarboxaldehyde) (Roddan et al., 2020). Thus, *NCS1* may be involved in other unknown metabolic pathways in *P. amurense*, and it is not exclusively specific to BIA biosynthesis. Additionally, the synthesis of plant secondary metabolites is often regulated by complex processes, particularly nitrogen-containing alkaloids (Yamada & Sato, 2021). The regulation of BIA synthesis is mediated by numerous transcription factors, such as the WRKY, bHLH, and ERF families (Kato et al., 2007; Yamada, Koyama, & Sato, 2011; Yamada et al., 2016). Plants initiate self-protection mechanisms to induce negative feedback regulation by transcription factors when they are stressed, resulting in the upregulation of certain structural genes to enhance the contents of particular compounds (Mu et al., 2023). Similarly, a comparable regulatory mechanism may exist for BIA synthesis in *P. amurense*. When (*S*)-norcoclaurine is reduced, negative regulators upregulate the expression of NCS by virtue of the absence of precursors dopamine, leading to an opposing trend of NCS expression levels and (*S*)-norcoclaurine content. Based on these results, a possible BIA biosynthetic pathway in *P. amurense* was proposed (Fig. 3B), although the actual catalytic functions of these genes require further investigation.

5. Conclusion

In this work, the *de novo* assembly of transcripts from 18 tissues of *P. amurense* was reported, and 28 targeted metabolites related to BIA biosynthesis were identified and quantified. A potential case of evolution involving MTs and CYP450 between *C. japonica* and *P. amurense* was found in the BIA biosynthetic pathway. The BIA biosynthetic pathway in non-Ranunculales species was presented, and 51 candidate enzyme genes, including 14 *CYP450s* and 33 *MTs*, were identified. Among them, a PR10/Bet v1 gene encoding NCS was verified to be the key enzyme contributing to the formation of (*S*)-norcoclaurine. These findings provide valuable clues to understanding the BIA biosynthesis in the distant lineage of Ranunculales species.

CRediT authorship contribution statement

Tingxia Liu: Formal analysis, Investigation, Visualization, Writing – original draft. **Wanran Zhang:** Formal analysis, Investigation, Visualization, Validation. **Sijia Wang:** Investigation, Validation. **Ya Tian:** Formal analysis. **Yifan Wang:** Formal analysis. **Ranran Gao:** Data curation. **Shilin Chen:** Project administration. **Wei Sun:** Resources, Data curation, Project administration. **Wei Ma:** Funding acquisition, Project administration, Writing – review & editing. **Zhichao Xu:** Conceptualization, Project administration, Writing – review & editing.

Declaration of competing interest

The authors declare that they have no known competing financial interests or personal relationships that could have appeared to influence the work reported in this paper.

Acknowledgments

This research was funded by grants from the National Key Research and Development Project "research and demonstration of collection, screening, and breeding technology of ginseng and other genuine medicinal materials" (No. 2021YFD1600901), National Natural Science Foundation of China (No. 82274037), and Heilongjiang Touyan Innovation Team Program (No. HLJTYTP2019001).

Appendix A. Supplementary material

All sequencing data are submitted to the NCBI Sequence Read Archive database with an accession number PRJNA859281. Supplementary material to this article can be found online at https://doi.org/10.1016/j.chmed.2024.11.003.

References

Bolger, A. M., Lohse, M., & Usadel, B. (2014). Trimmomatic: A flexible trimmer for Illumina sequence data. *Bioinformatics, 30*(15), 2114–2120.

Cao, M., Gao, M., Suástegui, M., Mei, Y., & Shao, Z. (2020). Building microbial factories for the production of aromatic amino acid pathway derivatives: From commodity chemicals to plant-sourced natural products. *Metabolic Engineering, 58*, 94–132.

Capella-Gutiérrez, S., Silla-Martínez, J. M., & Gabaldón, T. (2009). trimAl: A tool for automated alignment trimming in large-scale phylogenetic analyses. *Bioinformatics, 25*(15), 1972–1973.

Chi, P. T. L., Van Hung, P., Le Thanh, H., & Phi, N. T. L. (2020). Valorization of *Citrus* leaves: Chemical composition, antioxidant and antibacterial activities of essential oils. *Waste and Biomass Valorization, 11*(9), 4849–4857.

Chinese Pharmacopoeia and Commission. (2020). *Pharmacopoeia of the People's Republic of China*, Part 1. In C. P. a. Commission (Ed.). Beijing: Chinese Medical Science and Technology Press, 153.

Choi, K. B., Morishige, T., Shitan, N., Yazaki, K., & Sato, F. (2002). Molecular cloning and characterization of coclaurine *N*-methyltransferase from cultured cells of *Coptis japonica*. *Journal of Biological Chemistry, 277*(1), 830–835.

Cui, X., Meng, F., Pan, X., Qiu, X., Zhang, S., Li, C., & Lu, S. (2022). Chromosome-level genome assembly of *Aristolochia contorta* provides insights into the biosynthesis of benzylisoquinoline alkaloids and aristolochic acids. *Horticulture Research, 9*, uhac005.

Dang, T. T., & Facchini, P. J. (2012). Characterization of three *O*-methyltransferases involved in noscapine biosynthesis in opium poppy. *Plant Physiology, 159*(2), 618–631.

Deng, X., Zhao, L., Fang, T., Xiong, Y., Ogutu, C., Yang, D., ... Han, Y. (2018). Investigation of benzylisoquinoline alkaloid biosynthetic pathway and its transcriptional regulation in lotus. *Horticulture Research, 5*, 29.

Denoeud, F., Carretero-Paulet, L., Dereeper, A., Droc, G., Guyot, R., Pietrella, M., ... Lashermes, P. (2014). The coffee genome provides insight into the convergent evolution of caffeine biosynthesis. *Science, 345*(6201), 1181–1184.

Dulan, B., Wang, H., Wu, Y., Ling, L., & Anggelima (2022). Famous traditional Mongolian medicine xieriga-4 (turmeric-4) decoction: A review. *Chinese Herbal Medicines, 14*(3), 385–391.

Feng, S., Liu, Z., Cheng, J., Li, Z., Tian, L., Liu, M., ... Wei, A. (2021). *Zanthoxylum*-specific whole genome duplication and recent activity of transposable elements in the highly repetitive paleotetraploid *Z. bungeanum* genome. *Horticulture Research, 8*(1), 205.

Gao, R., Lou, Q., Hao, L., Qi, G., Tian, Y., Pu, X., ... Song, J. (2022). Comparative genomics reveal the convergent evolution of CYP82D and CYP706X members related to flavone biosynthesis in Lamiaceae and Asteraceae. *The Plant Journal, 109*(5), 1305–1318.

Gesell, A., Rolf, M., Ziegler, J., Díaz Chávez, M. L., Huang, F. C., & Kutchan, T. M. (2009). CYP719B1 is salutaridine synthase, the C-C phenol-coupling enzyme of morphine biosynthesis in opium poppy. *Journal of Biological Chemistry, 284*(36), 24432–24442.

Ghirga, F., Bonamore, A., Calisti, L., D'Acquarica, I., Mori, M., Botta, B., ... Macone, A. (2017). Green routes for the production of enantiopure benzylisoquinoline alkaloids. *International Journal of Molecular Sciences, 18*(11), 2464.

Grabherr, M. G., Haas, B. J., Yassour, M., Levin, J. Z., Thompson, D. A., Amit, I., ... Regev, A. (2011). Full-length transcriptome assembly from RNA-Seq data without a reference genome. *Nature Biotechnology, 29*(7), 644–652.

Guo, L., Winzer, T., Yang, X., Li, Y., Ning, Z., He, Z., ... Ye, K. (2018). The opium poppy genome and morphinan production. *Science, 362*(6412), 343–347.

Guo, W., Yan, H., Ren, X., Tang, R., Sun, Y., Wang, Y., & Feng, J. (2020). Berberine induces resistance against tobacco mosaic virus in tobacco. *Pest Management Science, 76*(5), 1804–1813.

Habtemariam, S. (2016). Berberine and inflammatory bowel disease: A concise review. *Pharmacological Research, 113*, 592–599.

Huang, F. C., & Kutchan, T. M. (2000). Distribution of morphinan and benzo [c] phenanthridine alkaloid gene transcript accumulation in *Papaver somniferum*. *Phytochemistry, 53*(5), 555–564.

Ikezawa, N., Tanaka, M., Nagayoshi, M., Shinkyo, R., Sakaki, T., Inouye, K., & Sato, F. (2003). Molecular cloning and characterization of CYP719, a methylenedioxy bridge-forming enzyme that belongs to a novel P450 family, from cultured *Coptis japonica* cells. *Journal of Biological Chemistry, 278*(40), 38557–38565.

Ilari, A., Franceschini, S., Bonamore, A., Arenghi, F., Botta, B., Macone, A., ... Boffi, A. (2009). Structural basis of enzymatic (*S*)-norcoclaurine biosynthesis. *Journal of Biological Chemistry, 284*(2), 897–904.

Ilyas, Z., Perna, S., Al-thawadi, S., Alalwan, T. A., Riva, A., Petrangolini, G., ... Rondanelli, M. (2020). The effect of berberine on weight loss in order to prevent obesity: A systematic review. *Biomedicine & Pharmacotherapy, 127*, 110137.

Imenshahidi, M., & Hosseinzadeh, H. (2019). Berberine and barberry (*Berberis vulgaris*): A clinical review. *Phytotherapy Research, 33*(3), 504–523.

Iwasa, K., Moriyasu, M., & Nader, B. (2000). Fungicidal and herbicidal activities of berberine related alkaloids. *Bioscience, Biotechnology, and Biochemistry, 64*(9), 1998–2000.

Jain, S., Tripathi, S., & Tripathi, P. K. (2023). Antioxidant and antiarthritic potential of berberine: *In vitro* and *in vivo* studies. *Chinese Herbal Medicines, 15*(4), 549–555.

Kato, N., Dubouzet, E., Kokabu, Y., Yoshida, S., Taniguchi, Y., Dubouzet, J. G., ... Sato, F. (2007). Identification of a WRKY protein as a transcriptional regulator of benzylisoquinoline alkaloid biosynthesis in *Coptis japonica*. *Plant & Cell Physiology, 48*(1), 8–18.

Katoh, K., Misawa, K., Kuma, K. I., & Miyata, T. (2002). MAFFT: A novel method for rapid multiple sequence alignment based on fast Fourier transform. *Nucleic Acids Research, 30*(14), 3059–3066.

Kim, S., Park, M., Yeom, S. I., Kim, Y. M., Lee, J. M., Lee, H. A., ... Choi, D. (2014). Genome sequence of the hot pepper provides insights into the evolution of pungency in *Capsicum* species. *Nature Genetics, 46*(3), 270–278.

Langfelder, P., & Horvath, S. (2008). WGCNA: An R package for weighted correlation network analysis. *BMC Bioinformatics, 9*, 559.

Li, X., Cai, K., Fan, Z., Wang, J., Wang, L., Wang, Q., ... Zhao, X. (2022). Dissection of transcriptome and metabolome insights into the isoquinoline alkaloid biosynthesis during stem development in *Phellodendron amurense* (Rupr.). *Plant Science, 325*, 111461.

Liang, W., Cheng, J., Zhang, J., Xiong, Q., Jin, M., & Zhao, J. (2022). pH-Responsive on-demand alkaloids release from core-shell ZnO@ZIF-8 nanosphere for synergistic control of bacterial wilt disease. *ACS Nano, 16*(2), 2762–2773.

Liscombe, D. K., MacLeod, B. P., Loukanina, N., Nandi, O. I., & Facchini, P. J. (2005). Evidence for the monophyletic evolution of benzylisoquinoline alkaloid biosynthesis in angiosperms. *Phytochemistry, 66*(11), 1374–1393.

Liu, D., Meng, X., Wu, D., Qiu, Z., & Luo, H. (2019). A natural isoquinoline alkaloid with antitumor activity: Studies of the biological activities of berberine. *Frontiers in Pharmacology, 10*, 9.

Luo, H., Li, Y., Sun, C., Wu, Q., Song, J., Sun, Y., ... Chen, S. (2010). Comparison of 454-ESTs from *Huperzia serrata* and *Phlegmariurus carinatus* reveals putative genes involved in lycopodium alkaloid biosynthesis and developmental regulation. *BMC Plant Biology, 10*, 209.

Manni, M., Berkeley, M. R., Seppey, M., Simão, F. A., & Zdobnov, E. M. (2021). BUSCO update: Novel and streamlined workflows along with broader and deeper phylogenetic coverage for scoring of eukaryotic, prokaryotic, and viral genomes. *Molecular Biology and Evolution, 38*(10), 4647–4654.

Minami, H., Dubouzet, E., Iwasa, K., & Sato, F. (2007). Functional analysis of norcoclaurine synthase in *Coptis japonica*. *Journal of Biological Chemistry, 282*(9), 6274–6282.

Minami, H., Kim, J. S., Ikezawa, N., Takemura, T., Katayama, T., Kumagai, H., & Sato, F. (2008). Microbial production of plant benzylisoquinoline alkaloids. *Proceedings of the National Academy of Sciences of the United States of America, 105*(21), 7393–7398.

Miyazawa, M., Fujioka, J., & Ishikawa, Y. (2002). Insecticidal compounds from *Phellodendron amurense* active against *Drosophila melanogaster*. *Journal of the Science of Food and Agriculture, 82*(8), 830–833.
Mizutani, M., & Sato, F. (2011). Unusual P450 reactions in plant secondary metabolism. *Archives of Biochemistry and Biophysics, 507*(1), 194–203.
Morishige, T., Tsujita, T., Yamada, Y., & Sato, F. (2000). Molecular characterization of the *S*-adenosyl-l-methionine: 3′-Hydroxy-*N*-methylcoclaurine 4′-*O*-methyltransferase involved in isoquinoline alkaloid biosynthesis in *Coptis japonica*. *Journal of Biological Chemistry, 275*(30), 23398–23405.
Mu, H., Li, Y., Yuan, L., Jiang, J., Wei, Y., Duan, W., ... Wang, L. (2023). MYB30 and MYB14 form a repressor-activator module with WRKY8 that controls stilbene biosynthesis in grapevine. *The Plant Cell, 35*(1), 552–573.
Nelson, D. R., Ming, R., Alam, M., & Schuler, M. A. (2008). Comparison of cytochrome P450 genes from six plant genomes. *Tropical Plant Biology, 1*(3), 216–235.
Ozturk, M., Chia, J. E., Hazra, R., Saqib, M., Maine, R. A., Guler, R., ... Parihar, S. P. (2021). Evaluation of berberine as an adjunct to TB treatment. *Frontiers in Immunology, 12*, 656419.
Pasquo, A., Bonamore, A., Franceschini, S., Macone, A., Boffi, A., & Ilari, A. (2008). Cloning, expression, crystallization and preliminary X-ray data analysis of norcoclaurine synthase from *Thalictrum flavum*. *Acta Crystallographica Section F, Structural Biology and Crystallization Communications, 64*(4), 281–283.
Pauli, H. H., & Kutchan, T. M. (1998). Molecular cloning and functional heterologous expression of two alleles encoding (*S*)-*N*-methylcoclaurine 3'-hydroxylase (CYP80B1), a new methyl jasmonate-inducible cytochrome P-450-dependent mono-oxygenase of benzylisoquinoline alkaloid biosynthesis. *Plant Journal, 13*(6), 793–801.
Roddan, R., Sula, A., Méndez-Sánchez, D., Subrizi, F., Lichman, B. R., Broomfield, J., ... Hailes, H. C. (2020). Single step syntheses of (1*S*)-aryl-tetrahydroisoquinolines by norcoclaurine synthases. *Communications Chemistry, 3*(1), 170.
Samanani, N., & Facchini, P. J. (2001). Isolation and partial characterization of norcoclaurine synthase, the first committed step in benzylisoquinoline alkaloid biosynthesis, from opium poppy. *Planta, 213*(6), 898–906.
Samanani, N., Liscombe, D. K., & Facchini, P. J. (2004). Molecular cloning and characterization of norcoclaurine synthase, an enzyme catalyzing the first committed step in benzylisoquinoline alkaloid biosynthesis. *Plant Journal, 40*(2), 302–313.
Sato, F. (2013). Characterization of plant functions using cultured plant cells, and biotechnological applications. *Bioscience, Biotechnology, and Biochemistry, 77*(1), 1–9.
Sheng, X., & Himo, F. (2019). Enzymatic pictet-spengler reaction: Computational study of the mechanism and enantioselectivity of norcoclaurine synthase. *Journal of the American Chemical Society, 141*(28), 11230–11238.
Tajiri, M., Yamada, R., Hotsumi, M., Makabe, K., & Konno, H. (2021). The total synthesis of berberine and selected analogues, and their evaluation as amyloid beta aggregation inhibitors. *European Journal of Medicinal Chemistry, 215*, 113289.
Tang, W., & Eisenbrand, G. (1992). Qingdai. In *Chinese Drugs of Plant Origin* (pp. 805–812). Springer Berlin Heidelberg.
Van de Peer, Y., Mizrachi, E., & Marchal, K. (2017). The evolutionary significance of polyploidy. *Nature Reviews Genetics, 18*(7), 411–424.
Vimolmangkang, S., Deng, X., Owiti, A., Meelaph, T., Ogutu, C., & Han, Y. (2016). Evolutionary origin of the *NCSI* gene subfamily encoding norcoclaurine synthase is associated with the biosynthesis of benzylisoquinoline alkaloids in plants. *Scientific Reports, 6*, 26323.
Wang, W., Li, Q., Liu, Y., & Chen, B. (2015). Ionic liquid-aqueous solution ultrasonic-assisted extraction of three kinds of alkaloids from *Phellodendron amurense* Rupr and optimize conditions use response surface. *Ultrasonics Sonochemistry, 24*, 13–18.
Wang, W., Zu, Y., Fu, Y., Reichling, J., Suschke, U., Nokemper, S., & Zhang, Y. (2009). *In vitro* antioxidant, antimicrobial and anti-herpes simplex virus type 1 activity of *Phellodendron amurense* Rupr. from China. *The American Journal of Chinese Medicine, 37*(1), 195–203.
Wang, Y., Tong, Q., Shou, J. W., Zhao, Z. X., Li, X. Y., Zhang, X. F., ... Jiang, J. D. (2017). Gut microbiota-mediated personalized treatment of hyperlipidemia using berberine. *Theranostics, 7*(9), 2443–2451.
Wendel, J. F. (2015). The wondrous cycles of polyploidy in plants. *American Journal of Botany, 102*(11), 1753–1756.
Weng, J. K., Akiyama, T., Bonawitz, N. D., Li, X., Ralph, J., & Chapple, C. (2010). Convergent evolution of syringyl lignin biosynthesis *via* distinct pathways in the lycophyte *Selaginella* and flowering plants. *The Plant Cell, 22*(4), 1033–1045.
Wink, M. (2015). Modes of action of herbal medicines and plant secondary metabolites. *Medicines, 2*(3), 251–286.
Xian, X., Sun, B., Ye, X., Zhang, G., Hou, P., & Gao, H. (2014). Identification and analysis of alkaloids in cortex *Phellodendron amurense* by high-performance liquid chromatography with electrospray ionization mass spectrometry coupled with photodiode array detection. *Journal of Separation Science, 37*(13), 1533–1545.
Yamada, Y., Koyama, T., & Sato, F. (2011). Basic helix-loop-helix transcription factors and regulation of alkaloid biosynthesis. *Plant Signaling & Behavior, 6*(11), 1627–1630.
Yamada, Y., & Sato, F. (2021). Transcription factors in alkaloid engineering. *Biomolecules, 11*(11), 1719.
Yamada, Y., Yoshimoto, T., Yoshida, S. T., & Sato, F. (2016). Characterization of the promoter region of biosynthetic enzyme genes involved in berberine biosynthesis in *Coptis japonica*. *Frontiers in Plant Science, 7*, 1352.
Yang, W., Su, Y., Dong, G., Qian, G., Shi, Y., Mi, Y., ... Sun, W. (2020). Liquid chromatography–mass spectrometry-based metabolomics analysis of flavonoids and anthraquinones in *Fagopyrum tataricum* L. Gaertn. (Tartary buckwheat) seeds to trace morphological variations. *Food Chemistry, 331*, 127354.
Yang, Y., Li, Y., Chen, Q., Sun, Y., & Lu, Z. (2019). WGDdetector: A pipeline for detecting whole genome duplication events using the genome or transcriptome annotations. *BMC Bioinformatics, 20*(1), 75.
Yi, L. T., Zhu, J. X., Dong, S. Q., Chen, M., & Li, C. F. (2021). Berberine exerts antidepressant-like effects *via* regulating miR-34a-synaptotagmin1/Bcl-2 axis. *Chinese Herbal Medicines, 13*(1), 116–123.
Yin, J., Ye, J., & Jia, W. (2012). Effects and mechanisms of berberine in diabetes treatment. *Acta Pharmaceutica Sinica B, 2*(4), 327–334.
Zhang, Y., Xu, L., Qiu, J., Sun, M., Xia, C., Zhou, Z., & Liu, T. (2014). Provenance variations in berberine content of *Phellodendron amurense*, a rare and endangered medicinal plant grown in Northeast China. *Scandinavian Journal of Forest Research, 29*(8), 725–733.